IBRO Neuroscience Reports 11 (2021) 1–7

Contents lists available at ScienceDirect

IBRO Neuroscience Reports

journal homepage: www.sciencedirect.com/journal/IBRO-Neuroscience-Reports

# Reversal of motor-skill transfer impairment by trihexyphenidyl and reduction of dorsolateral striatal cholinergic interneurons in *Dyt1* ΔGAG knock-in mice

Fumiaki Yokoi [a,*], Mai Tu Dang [b], Lin Zhang [a,c], Kelly M. Dexter [a], Iakov Efimenko [a], Shiv Krishnaswamy [a], Matthew Villanueva [a], Carly I. Misztal [a], Malinda Gerard [a], Patrick Lynch [a], Yuqing Li [a,*]

[a] *Norman Fixel Institute of Neurological Diseases, McKnight Brain Institute, and Department of Neurology, College of Medicine, University of Florida, Gainesville, FL 32610-0236, USA*

[b] *Division of Neurology, Children's Hospital of Philadelphia, Philadelphia, PA 19104, USA*

[c] *Department of Biomedical Sciences, Center for Brain Repair, Florida State University College of Medicine, Tallahassee, FL, USA*

ARTICLE INFO

*Keywords:*
Cholinergic interneuron
Dystonia
Rotarod
TorsinA
*TOR1A*
Motor learning

ABSTRACT

DYT-TOR1A or DYT1 early-onset generalized dystonia is an inherited movement disorder characterized by sustained muscle contractions causing twisting, repetitive movements, or abnormal postures. The majority of the DYT1 dystonia patients have a trinucleotide GAG deletion in *DYT1/TOR1A*. Trihexyphenidyl (THP), an antagonist for excitatory muscarinic acetylcholine receptor M1, is commonly used to treat dystonia. *Dyt1* heterozygous ΔGAG knock-in (KI) mice, which have the corresponding mutation, exhibit impaired motor-skill transfer. Here, the effect of THP injection during the treadmill training period on the motor-skill transfer to the accelerated rotarod performance was examined. THP treatment reversed the motor-skill transfer impairment in *Dyt1* KI mice. Immunohistochemistry showed that *Dyt1* KI mice had a significant reduction of the dorsolateral striatal cholinergic interneurons. In contrast, Western blot analysis showed no significant alteration in the expression levels of the striatal enzymes and transporters involved in the acetylcholine metabolism. The results suggest a functional alteration of the cholinergic system underlying the impairment of motor-skill transfer and the pathogenesis of DYT1 dystonia. Training with THP in a motor task may improve another motor skill performance in DYT1 dystonia.

## 1. Introduction

Motor-skill learning is broadly viewed to include steps that reflect encoding or consolidation of the memory so that the entire process can be thought to consist of the fast, slow, consolidation, re-consolidation, automatization, and retention phases (Luft and Buitrago, 2005). The phases of motor-skill learning can be divided into two discrete stages, with the initial acquisition stage marked by a rapid improvement in performance, which is then followed by a phase when improvement is more gradual. The efficiency of motor-skill learning is dependent on such factors as the disruption caused by interference and facilitation of sleep during which memory consolidation occurs (Brashers-Krug et al., 1996). Another factor that contributes to the facilitation of motor learning is the ability to transfer a skill acquired during the learning of one task onto the process of more efficiently acquiring a new yet similar task (Krakauer et al., 2005; Seidler, 2004; Zanone and Kelso, 1997).

DYT1 early-onset generalized torsion dystonia [DYT-TOR1A dystonia; dystonia 1; Online Mendelian Inheritance in Man (OMIM) identifier #128100] is an inherited movement disorder characterized by sustained muscle contractions causing twisting, repetitive movements, or

*Abbreviations:* ACh, acetylcholine; AChE, acetylcholinesterase; BSA, bovine serum albumin; ChAT, choline acetyltransferase; ChI, cholinergic interneuron; ChT, choline transporter; CI, confidence interval; DAB, 3,3′-diaminobenzidine; DF, degrees of freedom; *Dyt1* KI mice, *Dyt1* ΔGAG heterozygous knock-in mice; GAPDH, Glyceraldehyde-3-phosphate dehydrogenase; KO, knockout; LTD, long-term depression; n.s., not significant; PB, phosphate buffer; PBS, phosphate-buffered saline; PET, positron emission tomography; THP, trihexyphenidyl; TrkA, tropomyosin receptor kinase A; VAChT, vesicular acetylcholine transporter; WT, wild-type.

* Correspondence to: Department of Neurology, College of Medicine, University of Florida, PO Box 100236, Gainesville, FL 32610-0236, USA.
*E-mail addresses:* fumiaki.yokoi@neurology.ufl.edu (F. Yokoi), yuqingli@ufl.edu (Y. Li).

https://doi.org/10.1016/j.ibneur.2021.05.003
Received 27 January 2021; Received in revised form 6 March 2021; Accepted 31 May 2021
Available online 12 June 2021

abnormal postures, resulting in motor control and coordination deficits (Albanese et al., 2013; Breakefield et al., 2008). Most patients have a heterozygous in-frame deletion of trinucleotide (ΔGAG) in *DYT1/-TOR1A*, coding for torsinA (Ozelius et al., 1997). About one in three with the ΔGAG mutation develops dystonic symptoms. Non-symptomatic carriers of the *DYT1* gene mutation have an impairment in sequence learning (Carbon et al., 2011; Ghilardi et al., 2003). Anticholinergics are a major category of medications used for generalized dystonia (Fahn, 1983; Jankovic, 2006), suggesting a functional alteration in the cholinergic system. Among them, trihexyphenidyl (THP) is an antagonist for excitatory muscarinic acetylcholine receptor M1.

*Dyt1* ΔGAG heterozygous knock-in (KI) mice have the corresponding trinucleotide deletion mutation in the endogenous *Dyt1/Tor1a*. *Dyt1* KI mice exhibit the long-term depression (LTD) deficits in the cortico-striatal pathway (Dang et al., 2012), sustained contraction and co-contraction of agonist and antagonist muscles of hind limbs (DeAndrade et al., 2016), and motor deficits of the hind limbs in the beam-walking test (Dang et al., 2005). THP ameliorates these deficits. Although the *Dyt1* KI mice do not show overt dystonic symptoms, motor deficits in the beam-walking test have been reproduced in distinct batches of this line (Cao et al., 2010; Yokoi et al., 2012) and another KI mouse line (Liu et al., 2021; Song et al., 2012). Similar motor deficits were also reported in other genetic mouse models for DYT11 myoclonus-dystonia (Li et al., 2021; Xiao et al., 2017; Yokoi et al., 2006) and DYT12 rapid-onset dystonia with parkinsonism (DeAndrade et al., 2011; Isaksen et al., 2017; Sugimoto et al., 2014). Motor deficits were also reported in other genetic animal models as previously reviewed (Imbriani et al., 2020; Oleas et al., 2015, 2013; Richter and Richter, 2014). Moreover, *Dyt1* KI mice exhibit impaired motor-skill transfer (Yokoi et al., 2015b). In this report, a novel skill transfer task was developed to examine motor-skill learning in *Dyt1* KI mice. The motor task involved forcing mice to run on a treadmill with increasing speeds over a training period of 2 weeks. After the training period, they were tested on an accelerated rotarod. WT mice trained on the treadmill improved their rotarod performance in comparison to untrained WT mice with the treadmill belt turned off. On the other hand, treadmill training in *Dyt1* KI mice did not affect the overall latency to fall in the rotarod test. This report suggests that trained WT mice had enhanced learning abilities due to their previous training on the treadmill, whereas *Dyt1* KI mice were unable to transfer their skills. Although THP ameliorates motor coordination deficits in *Dyt1* KI mice (Dang et al., 2012), the effect of THP on motor-skill transfer is not clear.

Acetylcholine (ACh) plays an essential role in striatal function (Eskow Jaunarajs et al., 2015; Lim et al., 2014; Pisani et al., 2007). Choline acetyltransferase (ChAT) catalyzes ACh synthesis from the choline and acetyl group of acetyl-CoA in the cholinergic interneurons (ChIs) (Prado et al., 2013). ACh is transported into the presynaptic vesicle *via* vesicular acetylcholine transporter (VAChT). The striatal ChIs show spontaneous firing and release ACh. The released ACh binds M1-type muscarinic acetylcholine receptors on the striatal medium spiny neurons and induces metabolic cascade to depolarize the membrane potentials (Delmas and Brown, 2005). The mRNAs for muscarinic receptors M1 and M4 are expressed at high levels in the striatal medium spiny neurons (Yan et al., 2001). The activation of dorsomedial striatal M1-type muscarinic cholinergic receptors, but not M4-type muscarinic cholinergic receptors, facilitates the flexible shifting of response patterns by maintaining or learning a new choice pattern (McCool et al., 2008). ACh also inhibits the ChI firing through M2-type inhibitory muscarinic acetylcholine receptors on the ChIs as a feedback regulation mechanism. ACh is degraded to choline and acetate by acetylcholinesterase (AChE). The choline is transported into the ChIs by choline transporter (ChT) and recycled to synthesize ACh.

Here, the effect of THP on the impaired motor-skill transfer in *Dyt1* KI mice was measured. Furthermore, the striatal cholinergic system in *Dyt1* KI mice was characterized by anatomical and biochemical approaches.

## 2. Experimental procedures

### 2.1. Animals

All experiments were carried out in compliance with the USPHS Guide for Care and Use of Laboratory Animals and approved by the Institutional Animal Care and Use Committees of the University of Alabama at Birmingham and the University of Florida. *Dyt1* KI mice and their littermate wild-type (WT) mice were prepared and genotyped by PCR as described earlier (Dang et al., 2005; Yokoi et al., 2009). Since male *Dyt1* KI mice exhibited significant motor deficits in the previous studies, only male mice were used for the present experiments. A total of 119 adult male WT (n = 60) and *Dyt1* KI (n = 59) littermates was used [mean, 172 days of age; 95% confidence interval (CI), 159–185]. Mice were housed under a 12 hr light and 12 hr dark cycle with *ad libitum* access to food and water. The experiments were performed by investigators blind to the treatments and the genotypes.

### 2.2. THP injection and motor-skill transfer test

Thirty-nine mice were used for a saline-injected control experiment, *i.e.,* 10 WT mice and 10 *Dyt1* KI mice were used for no training, and 10 WT mice and 9 *Dyt1* KI mice were used for treadmill training. On the other hand, 40 mice were used to examine the effect of THP on the motor-skill transfer, *i.e.*, 10 WT mice and 10 *Dyt1* KI mice were used for no training, and 10 WT mice and 10 *Dyt1* KI mice were used for treadmill training. Saline or THP (DL-Trihexyphenidyl hydrochloride; Sigma Aldrich, T1516; 0.8 mg/kg in saline) solution was injected intraperitoneally two hours before training onset every other day (total seven injections).

The training group mice were trained for two weeks on the treadmill with daily training on weekdays only. The treadmill apparatus (Weslo) for humans was converted to one for mice with an eight-lane (7 × 20 cm/lane) rectangular wood box divider (Supplementary Fig. 1) suspended 1 cm above the running belt as previously described (Yokoi et al., 2015b). Acrylic beads strung from a thin wire were placed along each lane's back wall to serve as a non-noxious stimulus for running. The treadmill was started at a running speed of approximately 13 m/min (0.5 mph) for 5 min each day. When more than 90% of the mice could run comfortably at that speed, it was increased by approximately 2.5 m/min (0.1 mph) to a maximum rate of about 18.5 m/min (0.7 mph). The mouse groups with no training were placed on the treadmill for 5 min each day, but the treadmill turned off.

After rest for two days, all mice were tested on an accelerating rotarod (Ugo Basile). It was started at 4 rpm with acceleration at a rate of 0.2 rpm/sec to a final speed of 28 rpm and a cutoff of 2 min as previously described (DeAndrade et al., 2011). Mice were tested with three trials each day for two consecutive days. The latency (seconds; s) to fall off the rotarod was measured for each mouse. Comparisons were made between WT or *Dyt1* KI mice with and without treadmill training and in saline- or THP-injected groups.

### 2.3. Immunohistochemistry

Frozen brain sections were prepared as described earlier to count the striatal ChI numbers (Yokoi et al., 2020b). The mice were anesthetized and perfused with ice-cold 0.1 M phosphate-buffered saline (pH 7.4; PBS) followed by 4% paraformaldehyde in 0.1 M phosphate buffer (pH 7.4; PB). The brains were dissected and incubated in 4% paraformaldehyde in 0.1 M phosphate buffer at 4 °C overnight. The brains were then incubated in 30% sucrose in 0.1 M PB at 4 °C overnight until the brains sank. The brains were frozen using dry-ice powder and cut into 40 μm thick coronal sections with a Histoslide 2000 sliding microtome (Reichert-Jung). The sections were obtained from 6 *Dyt1* KI and 8 WT littermates. Every sixth section was stained with goat anti-ChAT antibody (EMD Millipore, AB144P; 1:100 dilution) with

Vectastain ABC kit for peroxidase goat IgG and 3,3′-diaminobenzidine (DAB) peroxidase substrate kit (Vector laboratories). The ZEISS Axiophot RZGF-1 microscope with the Neurolucida program captured the images. The striatal area of the image was quadrisected by the ImageJ program to dorsolateral (DL), dorsomedial (DM), ventral lateral (VL), and ventral medial (VM) areas. It was vertically bisected at the midpoint of the corpus callosum and horizontally bisected halfway between the corpus callosum and the anterior commissure as described by others (Pappas et al., 2015). The collected slices contained the striata corresponding to the brain atlas from Bregma − 1.22 to 1.34 mm (Franklin and Paxinos, 2008). The number of ChAT-positive neurons was counted in the entire striatal regions of all stained sections (mean, 3 sections per mouse; 95% CI, 2–4 sections), and the area size was measured by the ImageJ program. The ChI density was calculated in total and each quadrant area and expressed as the number of ChIs per $mm^2$.

### 2.4. Western blot analysis

Two groups of mice were used for Western blot analysis. The first group had 7 WT and 7 *Dyt1* KI mice. The second group had 6 WT and 6 *Dyt1* KI mice. The striata were dissected, and the proteins were extracted in 1% Triton X-100-containing buffer as previously described (Yokoi et al., 2010). Each sample with 40 μg of proteins was separated on sodium dodecyl sulfate 10% polyacrylamide gel electrophoresis and transferred to Millipore Immobilon–FL transfer PVDF membranes. Western blot analysis was performed in duplicate as previously described (Yokoi et al., 2020b). The PVDF membranes were blocked with LI-COR Odyssey blocking buffer and incubated at 4°C overnight with goat anti-ChAT antibody (EMD Millipore, AB144P; 1:1000 dilution), goat anti-VAChT antibody (EMD Millipore, ABN100; 1:1000 dilution), rabbit anti-AChE antibody (Santa Cruz, sc-11409; 1000 dilution), rabbit anti-Tropomyosin receptor kinase A (TrkA) antibody (Advanced Targeting Systems, AB-N03; 1:1000 dilution), rabbit anti-ChT antibody (EMD Millipore, ABN458; 1:1000 dilution), rabbit anti-glyceraldehyde-3-phosphate dehydrogenase (GAPDH) antibody (Santa Cruz, sc-25778; 1:1000 dilution), rabbit β-tubulin (Cell signaling; #2128S; 1:1000 dilution) or goat β-tubulin antibody (Santa Cruz, sc-9935; 1:5833 dilution). LI-COR IRDye 800CW donkey anti-goat IgG (H+L) or LI-COR IRDye 680RD donkey anti-rabbit IgG (H+L) were used as the secondary antibodies as appropriate at dilution of 1:15,556. The infrared emission signals were detected and recorded as digital data by an LI-COR Odyssey imaging system. All Western blot data used in this manuscript were not saturated. Each band's density was normalized to the corresponding control, *i.e.*, GAPDH or β-tubulin, respectively.

### 2.5. Statistics

The latency to fall in the accelerated rotarod test was stratified by saline- or THP-injected condition and analyzed using SAS University Edition software GENMOD Procedure with GEE model and a negative binomial distribution concerning the body weight, age, and genotype as variables. The density of the striatal ChIs was analyzed by a generalized linear mixed-effects model (R program ver. 3.5.3; R Foundation for Statistical Computing, Vienna, Austria; glmmML) for the animal-based nested ChI number in Poison distribution concerning the offset log area size of the quadrant, age, the anterior-posterior slice position, and genotype as variables. The measured area size was analyzed by a linear mixed-effects model (R; lme) for the animal-based nested area size concerning age, anterior-posterior slice position, and genotype as variables. The Western blot data were analyzed by the R; lme program for the animal-based nested signal ratio concerning age and genotype as a variable. CI was calculated by the R; CI program. Significance was assigned at $p < 0.05$.

## 3. Results

### 3.1. Reversal of motor-skill transfer impairment in Dyt1 KI mice by THP

*Dyt1* KI mice show impaired motor-skill transfer (Yokoi et al., 2015b). THP is an antagonist of M1-type muscarinic acetylcholine receptors and is commonly used for dystonia patients. Here, the effect of THP on the impaired motor-skill transfer was examined by injecting either THP or saline every other day during the treadmill training period (Fig. 1A). The training group was forced to run on the treadmill for 5 min each weekday for 2 weeks. The No-training group was put on the static treadmill belt. After 2 days of resting, the motor-skill transfer performance was assayed on accelerated rotarod 3 trials per day for two days.

In the saline-injected group (Fig. 1B), WT mice with treadmill training stayed about 47% longer on the rotarod than WT mice without the training [mean ± standard errors (s); No training: 36.2 ± 4.3; n = 10; Training: 53.3 ± 6.4; n = 10; Z = 2.51; $p = 0.012$]. On the other hand, *Dyt1* KI mice did not show enhanced performance on rotarod with treadmill training (No training: 54.8 ± 5.2; n = 10; Training: 46.5 ± 5.2; n = 9; Z = −1.12; $p = 0.26$). The results were the same as previously reported without any injection (Yokoi et al., 2015b), suggesting that the vehicle injections do not affect the motor-skill transfer performance in both genotypes. On the other hand, the latency to fall in the accelerated rotarod test without training was not statistically different between WT and *Dyt1* KI mice in the saline-injected group (Z = 1.62; $p = 0.11$).

In the THP-injected group (Fig. 1C), WT mice with treadmill training stayed 55% longer on the accelerated rotarod than WT mice without treadmill training (No training: 44.0 ± 4.3; n = 10; Training: 68.3 ± 5.4; n = 10; Z = 3.47; $p = 0.0005$). This result reproduced the corresponding performance in the saline-injected WT mice, suggesting that THP did not affect the motor-skill transfer performance in WT mice. In contrast to the saline-injected *Dyt1* KI group, THP-injected *Dyt1* KI mice achieved 36% longer latency in accelerated performance after treadmill training than THP-injected *Dyt1* KI mice without treadmill training (No training: 53.0 ± 6.1; n = 10; Training: 72.1 ± 6.9; n = 10; Z = 2.02; $p = 0.044$). The results suggest that muscarinic acetylcholine receptor blockade during the treadmill training affected motor learning acquisition and restored the impaired motor-skill transfer in *Dyt1* KI mice.

### 3.2. Reduction of the dorsolateral striatal ChI density in Dyt1 KI mice

To dissect the mechanism of THP on motor skill transfer, we counted the number of the striatal ChIs in the coronal brain sections by ChAT immunohistochemistry in *Dyt1* KI mice (Fig. 2A, B). Since the ChIs are not evenly distributed in the striatum, the ChAT-positive neuron density was analyzed in each quadrant area (Pappas et al., 2018) of the striatum. The ChAT-positive neuron density in each quadrant area was obtained from WT (183 areas/8 mice) and *Dyt1* KI littermates (142 areas/6 mice). *Dyt1* KI mice showed a significant reduction of ChAT-positive neuron density in the dorsolateral striatum [ChI density (ChI numbers per $mm^2$) ± standard errors; WT, 21.4 ± 3.6; *Dyt1* KI, 11.0 ± 4.3; z(DF; 77) = − 2.02, $p = 0.044$; Fig. 2C, DL]. On the other hand, there was no significant difference in the ChAT-positive neuron densities between WT and *Dyt1* KI mice in the dorsomedial [WT, 30.3 ± 5.1; *Dyt1* KI, 22.5 ± 5.1; z(76) = − 1.14, $p = 0.25$; Fig. 2C, DM] or the ventrolateral striatum [WT, 21.2 ± 5.4; *Dyt1* KI, 13.5 ± 4.8; z(77) = − 1.43, $p = 0.15$; Fig. 2C, VL]. There were trends of reduction of the ChAT-positive neuron density in the ventromedial striatum [WT, 25.0 ± 4.2; *Dyt1* KI, 16.2 ± 2.7; z(76) = −1.68, $p = 0.093$; Fig. 2C, VM], and when all quadrants were analyzed together [WT, 27.9 ± 4.7; *Dyt1* KI, 19.2 ± 3.8; z(320) = − 1.73, $p = 0.084$; Fig. 2C, Str]. On the other hand, there was no significant difference in the measured area sizes of the quadrants between WT and *Dyt1* KI mice [mean ± standard errors ($mm^2$); DL, WT, 0.37 ± 0.01; *Dyt1* KI, 0.35 ± 0.02; t(11) = −

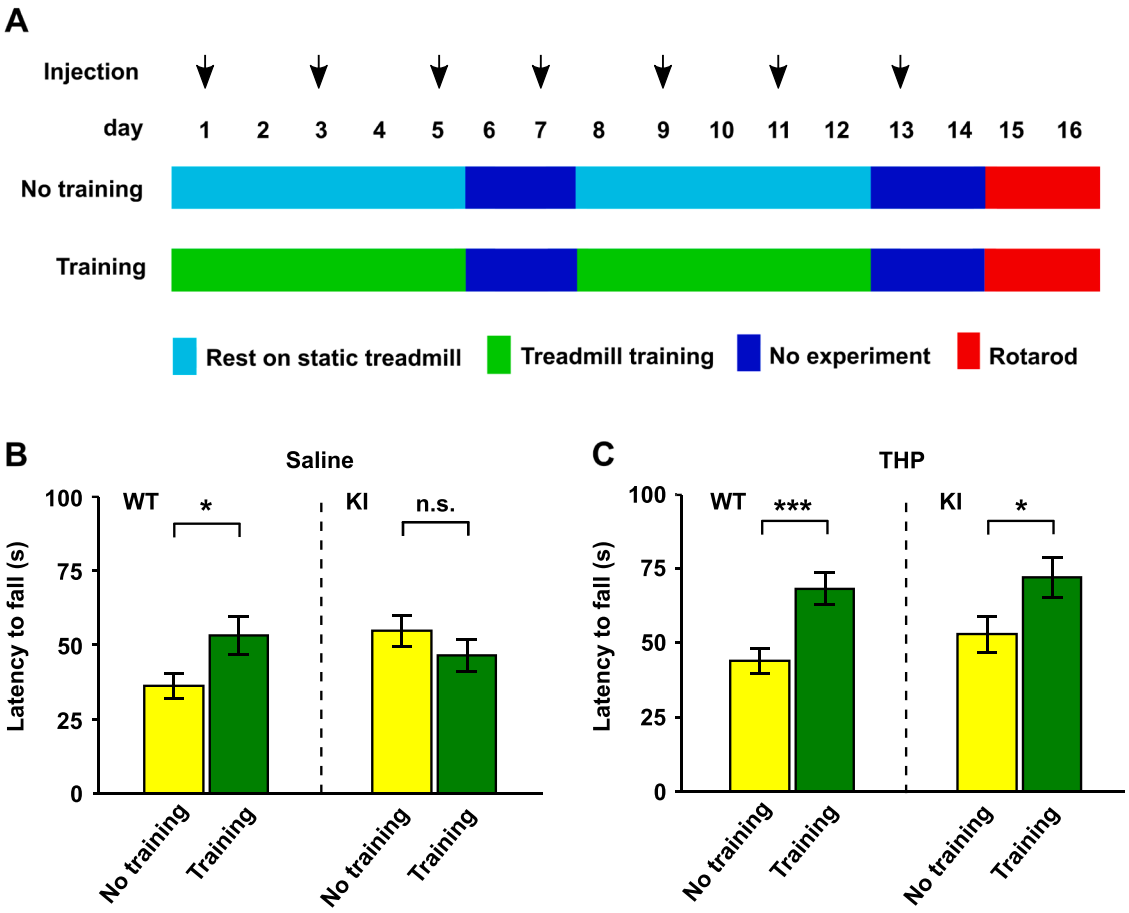


**Fig. 1.** Motor-skill transfer from treadmill training to accelerated rotarod test. **(A)** The time scheme of saline- or THP-injection (the arrows show injection days), resting (light blue bars) on the static treadmill belt, treadmill training (light green), and accelerated rotarod test (red bars). The dark blue bars indicate no behavioral experiments. **(B)** Motor-skill transfer in saline-injected mice. WT mice showed improved performance on the accelerated rotarod after treadmill training. In contrast, *Dyt1* KI mice failed to show motor-skill transfer as previously reported without saline injection. **(C)**. Motor-skill transfer with THP injection. Both WT and *Dyt1* KI mice showed increased latency to fall after treadmill training with THP injections, suggesting no side effect in WT and recovery from the impaired motor-skill transfer in *Dyt1* KI mice by THP, respectively. The bar graphs represent means ± standard errors of latency to fall. $*p < 0.05$; $***p < 0.001$; n.s.: not significant.

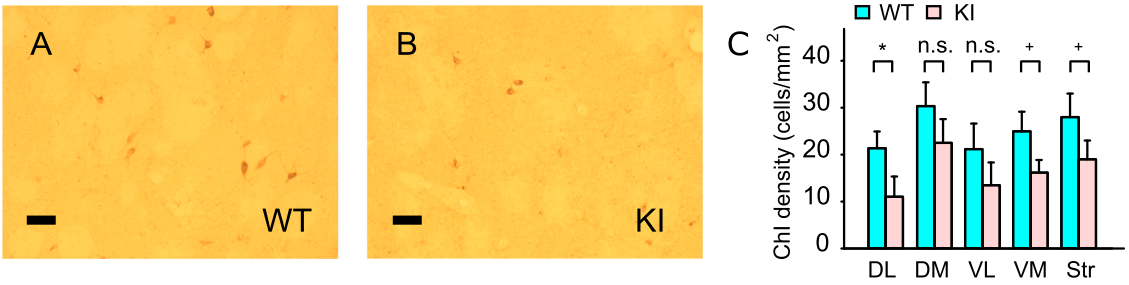


**Fig. 2.** Immunohistochemistry of the striatal ChIs. Representative images of the ChAT-positive cells in WT **(A)** and *Dyt1* KI **(B)** mice. Scale bars represent 50 μm. **(C)** There was a significant reduction of the ChI density in the dorsolateral (DL) striatum. The bar graphs indicate means ± standard errors of the ChI densities (ChAT-positive cell numbers/mm$^2$). $^+p < 0.1$; $*p < 0.05$; n.s.: not significant.

1.14, $p = 0.28$; DM, WT, 0.50 ± 0.01; *Dyt1* KI, 0.46 ± 0.02; t(11) = − 0.61, $p = 0.55$; VL, WT, 0.60 ± 0.02; *Dyt1* KI, 0.58 ± 0.02; t(11) = − 0.20, $p = 0.84$; VM, WT, 0.44 ± 0.02; *Dyt1* KI, 0.46 ± 0.02; t(11) = 0.62, $p = 0.54$; averaged quadrant size, WT, 0.48 ± 0.01; *Dyt1* KI, 0.46 ± 0.01; t(11) = − 0.49, $p = 0.63$]. The results suggest a reduction of the striatal ChI density in *Dyt1* KI mice, at least in the dorsolateral striatum.

### 3.3. No significant alteration of the striatal cholinergic enzyme or transporter levels in Dyt1 KI mice

The striatal ACh metabolic enzyme levels were further analyzed by Western blot. The *Dyt1* KI mice did not show significant differences in the striatal ChAT [normalized levels ± standard errors; WT: 100 ± 5.5%; *Dyt1* KI: 97.0 ± 4.2%; n = 6 each; t(DF: 9) = − 0.24, $p = 0.81$; Fig. 3A], VAChT [WT: 100 ± 5.7%; *Dyt1* KI: 108.3 ± 6.5%; n = 7 each; t(11) = 0.80, $p = 0.44$; Fig. 3B], ChT [75 kDa; WT: 100 ± 3.7%; *Dyt1* KI: 97.8 ± 2.7%; n = 7 each; t(11) = 0.07, $p = 0.95$;

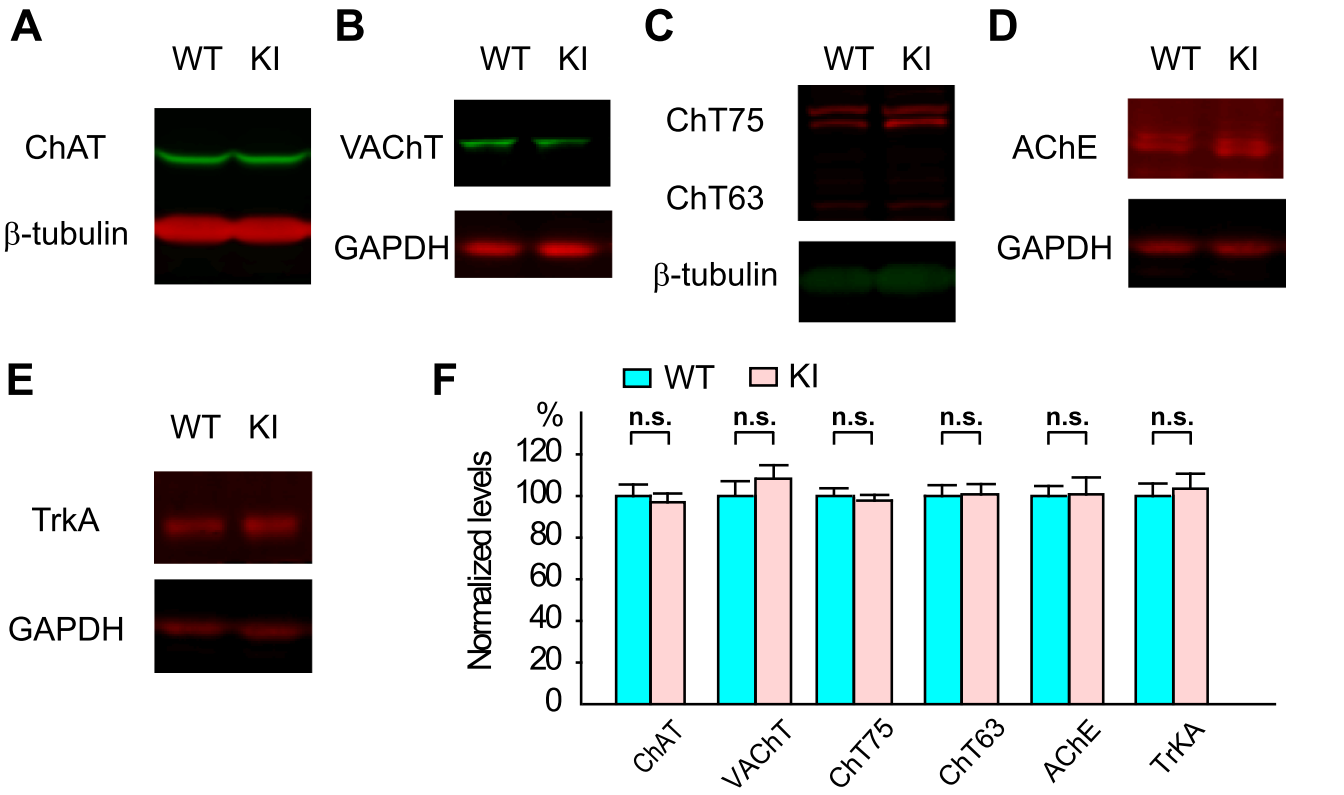


**Fig. 3.** Western blot analysis of the striatal tissues. The representative images for ChAT **(A)**, VAChT **(B)**, ChT (double bands at 75 kDa and a single band at 63 kDa; **C)**, AChE **(D)**, and TrkA **(E)** are shown. **(F)** The quantified signal of each protein was normalized with those of the loading control proteins, *i.e.*, β-tubulin or GAPDH. There was no significant difference in the ACh metabolic enzymes, transporters, or another ChI marker protein (TrkA) between WT and *Dyt1* KI mice. The bar graphs indicate means ± standard errors of the normalized signals. n.s.: not significant.

63 kDa; WT: 100 ± 5.2%; *Dyt1* KI: 100.8 ± 4.9%; n = 7 each; t(11) = 0.40, $p = 0.70$; Fig. 3C], and AChE [WT: 100 ± 4.8%; *Dyt1* KI: 100.8 ± 8.1%; n = 6 each; t(9) = 0.16, $p = 0.88$,; Fig. 3D]. These results suggest that there is no significant alteration in the levels of striatal ACh metabolic enzymes or transporters in *Dyt1* KI mice. Since TrkA, a neurotrophic receptor, is highly expressed in the striatal ChIs, it has been used as another marker of striatal ChIs (Sobreviela et al., 1994). The expression level of the striatal TrkA was further quantified. *Dyt1* KI mice did not show significant difference in the striatal TrkA level [WT: 100 ± 6.0%; *Dyt1* KI: 103.5 ± 7.2%; n = 6 each; t(9) = 0.47, $p = 0.65$, Fig. 3E]. Overall, there was no significant alteration in the striatal ACh metabolic or ChI marker enzyme levels in *Dyt1* KI mice (Fig. 3F).

## 4. Discussion

*Dyt1* KI mice exhibit impaired motor-skill transfer, lack of corticostriatal LTD, and motor coordination deficits such as beam walking and rotarod (Dang et al., 2012, 2005; Liu et al., 2021; Song et al., 2012; Yokoi et al., 2015b). The beam walking and corticostriatal LTD deficits can be reversed with THP treatment (Dang et al., 2012). Here, THP reversed the impaired motor-skill transfer in *Dyt1* KI mice, suggesting that a functional alteration of the cholinergic system contributes to the performance. *Dyt1* KI mice had a significantly reduced density of dorsolateral striatal ChIs, whereas there was no significant alteration in the striatal cholinergic enzyme or transporter levels. The present results indicate that complex changes in the striatal cholinergic system might underlie the impaired motor-skill transfer and the pathogenesis of DYT1 dystonia. A limitation in the present study is no direct evidence showing that the reduction of dorsolateral cholinergic interneurons contributes to the impaired motor skill transfer in *Dyt1* KI mice. The results shown in Figs. 1 and 2 suggest functional alterations of the cholinergic system or its relating pathways contribute to the impaired motor skill transfer in *Dyt1* KI mice. On the other hand, Fig. 3 suggests no significant alteration in the striatal ACh metabolism. One possible mechanism is that the remaining striatal ChIs increased their ACh metabolism to compensate for the low number of ChIs. Therefore the ACh metabolism per ChI may be relatively increased, and this may produce abnormal, hyperactive local ChI circuits.

While the treadmill and rotarod are two separate tests, they are similar in forced running and adaptation to the speed. However, the rotarod has an added challenge of keeping balance on the rotating rod and is different from treadmill running on a flat moving belt. From the neuronal activity perspective, this skill transfer could represent prior priming of the neuronal circuitry involved in learning to facilitate further learning. The present results show that THP injection during the treadmill training period reverses the impaired motor-skill transfer in *Dyt1* KI mice, suggesting that THP affects the acquisition phase of motor-skill learning. THP ameliorates the corticostriatal LTD, motor deficits, and abnormal muscle contractions in *Dyt1* KI mice (Dang et al., 2012; DeAndrade et al., 2016). Consistent with these findings, striatal levels of ACh are elevated in KI mice (Scarduzio et al., 2017). Moreover, a recent paper suggests that THP stimulates the striatal ChI and increases ACh release. The released ACh stimulates nicotinic receptors on the dopaminergic neurons and increases dopamine release (Downs et al., 2019). One possible cellular mechanism is that THP restores corticostriatal LTD deficits during the treadmill training period and enhances motor-skill learning acquisition.

Most studies suggest that there is no overt neurodegeneration in DYT1 dystonia patients (Breakefield et al., 2008). Consistently, there is no overt neurodegeneration in *Dyt1* KI mice (Dang et al., 2005). On the other hand, there is a subtle morphological alteration in the cerebellar Purkinje cells in *Dyt1* KI mice (Zhang et al., 2011) and another KI mouse line (Song et al., 2014). The amygdala's central nucleus' size is significantly reduced in the KI mice (Yokoi et al., 2009). Moreover, another KI

mouse line of torsinA shows mostly normal density of striatal ChI except an increased ChI density in the dorsolateral striatum (Song et al., 2013). In contrast to the other KI mice, the present study showed a significant reduction of the dorsolateral striatal ChIs in *Dyt1* KI mice, consistent with the reduced trkA expression in postmortem tissues from older DYT1 dystonia patients (Pappas et al., 2015). Moreover, a recent study using positron emission tomography (PET) suggests a decrease in VAChT expression in the posterior putamen and caudate nucleus of young DYT1 dystonia patients (Mazere et al., 2021). On the other hand, *Dyt1* KI mice showed normal levels of striatal cholinergic enzymes and TrkA. Since the detected protein levels from the total spiritual tissues does not reflect the local cholinergic metabolism in each quadrant, the normal Western blot data is mostly consistent with no significant alteration of total ChI density in the combined striatal areas. Moreover, the surviving ChI neurons may upregulate the expression levels to compensate for the partial loss of striatal ChIs. Overall, the results suggest that the anatomical and biochemical properties of the striatal ChIs in *Dyt1* KI mice was mostly normal except for the reduction of ChIs in the dorsolateral region. Dorsolateral striatum is known to engage motor skill learning (Yin et al., 2009). The functional alteration of the local striatal cholinergic system may contribute to impairment of the motor skill transfer.

In contrast to the lethality in the complete torsinA loss mouse models (Goodchild et al., 2005; Yokoi et al., 2008), the partial loss of torsinA function models, such as *Dyt1* knockdown (Dang et al., 2006) and *Dyt1* heterozygous KO mice (Yokoi et al., 2015a), show motor deficits in the beam-walking test. The striatum-specific *Dyt1* conditional knockout mice also show motor deficits (Yokoi et al., 2011). Moreover, the cerebral cortex-specific *Dyt1* conditional knockout mice show motor deficit without overt developmental alteration in cerebral cortex neurons (Yokoi et al., 2008). On the other hand, dopamine receptor 2-expressing-cell specific *Dyt1* conditional KO (*Dyt*1 d2KO) mice show decreased striatal ChIs and motor deficits (Yokoi et al., 2020b). Moreover, Dlx-CKO mice, which have a combination of the heterozygous KO and *Dlx5/6-Cre*-derived conditional KO in the forebrain neurons, show a severe reduction of the dorsal striatal ChIs (Pappas et al., 2015). Similarly, the present results showed *Dyt1* KI mice had reduced dorsolateral striatal ChIs. Since *Dyt*1 KI mice express reduced striatal torsinA (Yokoi et al., 2010), these phenotypes may be caused by a partial loss of torsinA function in *Dyt1* KI mice. It should be noted that nestin-expressing cell-specific conditional KO mice show complete infant lethality and neurodegeneration in multiple brain regions (Liang et al., 2014). However, overt neurodegeneration and complete lethality seem to be caused by malnutrition due to the failure of the mutant mice competing for food (Yokoi et al., 2020a). These previous studies and the present results support a relationship between the loss of torsinA function and the neurodegeneration, especially the ChIs, in the pathogenesis of DYT1 dystonia.

## CRediT authorship contribution statement

**Fumiaki Yokoi:** Conceptualization, Methodology, Investigation, Formal analysis, Writing - original draft, Visualization, Supervision, Funding acquisition, **Mai Tu Dang**: Conceptualization, Methodology, Writing - original draft, **Lin Zhang**: Investigation, **Kelly M. Dexter:** Investigation, **Iakov Efimenko:** Investigation, **Shiv Krishnaswamy:** Investigation, **Matthew Villanueva:** Investigation, **Carly I. Misztal:** Investigation, **Malinda Gerard:** Investigation, **Patrick Lynch:** Investigation, **Yuqing Li:** Conceptualization, Formal analysis, Resources, Writing - review & editing, Supervision, Funding acquisition.

## Conflicts of Interest

The authors declare no competing financial interests.

## Acknowledgment

We thank Andrea McCullough and their staff for animal care, Miki Jinno, Jessica Artille, Jareisha Vickers, Aysha Awal, Alyka Glor Fernandez, and other undergraduate students for their technical assistance. This work was supported by Tyler's Hope for a Dystonia Cure, Inc., "Mini-Moonshot" Fixel-MBI Pilot Grant Mechanism for Dystonia and Related Disorders, National Institutes of Health (NS54246, NS72782, NS75012, NS82244, NS111498, and NS118397), startup funds from the Department of Neurology (UAB and UF), Dystonia Medical Research Foundation, and Bachmann-Strauss Dystonia and Parkinson Foundation, Inc., and Department of Defense (W81XWH1810099). FY was partially supported by the Office of the Assistant Secretary of Defense for Health Affairs through the Peer-Reviewed Medical Research Program Discovery Award. Opinions, interpretations, conclusions, and recommendations are those of the author and are not necessarily endorsed by the Department of Defense.

### *Ethical Statement*

The authors declare no competing financial interests.

## Appendix A. Supporting information

Supplementary data associated with this article can be found in the online version at doi:10.1016/j.ibneur.2021.05.003.

## References

Albanese, A., Bhatia, K., Bressman, S.B., Delong, M.R., Fahn, S., Fung, V.S., Hallett, M., Jankovic, J., Jinnah, H.A., Klein, C., Lang, A.E., Mink, J.W., Teller, J.K., 2013. Phenomenology and classification of dystonia: a consensus update. Mov. Disord. 28, 863–873.

Brashers-Krug, T., Shadmehr, R., Bizzi, E., 1996. Consolidation in human motor memory. Nature 382, 252–255.

Breakefield, X.O., Blood, A.J., Li, Y., Hallett, M., Hanson, P.I., Standaert, D.G., 2008. The pathophysiological basis of dystonias. Nat. Rev. Neurosci. 9, 222–234.

Cao, S., Hewett, J.W., Yokoi, F., Lu, J., Buckley, A.C., Burdette, A.J., Chen, P., Nery, F.C., Li, Y., Breakefield, X.O., Caldwell, G.A., Caldwell, K.A., 2010. Chemical enhancement of torsinA function in cell and animal models of torsion dystonia. Dis. Models Mech. 3, 386–396.

Carbon, M., Argyelan, M., Ghilardi, M.F., Mattis, P., Dhawan, V., Bressman, S., Eidelberg, D., 2011. Impaired sequence learning in dystonia mutation carriers: a genotypic effect. Brain 134, 1416–1427.

Dang, M.T., Yokoi, F., Cheetham, C.C., Lu, J., Vo, V., Lovinger, D.M., Li, Y., 2012. An anticholinergic reverses motor control and corticostriatal LTD deficits in Dyt1 DeltaGAG knock-in mice. Behav. Brain Res. 226, 465–472.

Dang, M.T., Yokoi, F., McNaught, K.S., Jengelley, T.A., Jackson, T., Li, J., Li, Y., 2005. Generation and characterization of Dyt1 DeltaGAG knock-in mouse as a model for early-onset dystonia. Exp. Neurol. 196, 452–463.

Dang, M.T., Yokoi, F., Pence, M.A., Li, Y., 2006. Motor deficits and hyperactivity in Dyt1 knockdown mice. Neurosci. Res. 56, 470–474.

DeAndrade, M.P., Trongnetrpunya, A., Yokoi, F., Cheetham, C.C., Peng, N., Wyss, J.M., Ding, M., Li, Y., 2016. Electromyographic evidence in support of a knock-in mouse model of DYT1 Dystonia. Mov. Disord. 31, 1633–1639.

DeAndrade, M.P., Yokoi, F., van Groen, T., Lingrel, J.B., Li, Y., 2011. Characterization of Atp1a3 mutant mice as a model of rapid-onset dystonia with parkinsonism. Behav. Brain Res. 216, 659–665.

Delmas, P., Brown, D.A., 2005. Pathways modulating neural KCNQ/M (Kv7) potassium channels. Nat. Rev. Neurosci. 6, 850–862.

Downs, A.M., Fan, X., Donsante, C., Jinnah, H.A., Hess, E.J., 2019. Trihexyphenidyl rescues the deficit in dopamine neurotransmission in a mouse model of DYT1 dystonia. Neurobiol. Dis. 125, 115–122.

Eskow Jaunarajs, K.L., Bonsi, P., Chesselet, M.F., Standaert, D.G., Pisani, A., 2015. Striatal cholinergic dysfunction as a unifying theme in the pathophysiology of dystonia. Prog. Neurobiol. 127–128, 91–107.

Fahn, S., 1983. High dosage anticholinergic therapy in dystonia. Neurology 33, 1255–1261.

Franklin, K.B.J., Paxinos, G., 2008. The Mouse Brain in stereotaxic coordinates, Third ed. Elsevier Inc, San Diego.

Ghilardi, M.F., Carbon, M., Silvestri, G., Dhawan, V., Tagliati, M., Bressman, S., Ghez, C., Eidelberg, D., 2003. Impaired sequence learning in carriers of the DYT1 dystonia mutation. Ann. Neurol. 54, 102–109.

Goodchild, R.E., Kim, C.E., Dauer, W.T., 2005. Loss of the dystonia-associated protein torsinA selectively disrupts the neuronal nuclear envelope. Neuron 48, 923–932.

Imbriani, P., Ponterio, G., Tassone, A., Sciamanna, G., El Atiallah, I., Bonsi, P., Pisani, A., 2020. Models of dystonia: an update. J. Neurosci. Methods 339, 108728.

Isaksen, T.J., Kros, L., Vedovato, N., Holm, T.H., Vitenzon, A., Gadsby, D.C., Khodakhah, K., Lykke-Hartmann, K., 2017. Hypothermia-induced dystonia and abnormal cerebellar activity in a mouse model with a single disease-mutation in the sodium-potassium pump. PLoS Genet. 13, 1006763.
Jankovic, J., 2006. Treatment of dystonia. Lancet Neurol. 5, 864–872.
Krakauer, J.W., Ghez, C., Ghilardi, M.F., 2005. Adaptation to visuomotor transformations: consolidation, interference, and forgetting. J. Neurosci. 25, 473–478.
Li, J., Liu, Y., Li, Q., Huang, X., Zhou, D., Xu, H., Zhao, F., Mi, X., Wang, R., Jia, F., et al., 2021. Mutation in ε-Sarcoglycan induces a Myoclonus-Dystonia syndrome-like movement disorder in mice. Neurosci. Bull. 37, 311–322.
Liang, C.C., Tanabe, L.M., Jou, S., Chi, F., Dauer, W.T., 2014. TorsinA hypofunction causes abnormal twisting movements and sensorimotor circuit neurodegeneration. J. Clin. Investig. 124, 3080–3092.
Lim, S.A., Kang, U.J., McGehee, D.S., 2014. Striatal cholinergic interneuron regulation and circuit effects. Front. Synaptic Neurosci. 6, 22.
Liu, Y., Xing, H., Yokoi, F., Vaillancourt, D.E., Li, Y., 2021. Investigating the role of striatal dopamine receptor 2 in motor coordination and balance: insights into the pathogenesis of DYT1 dystonia. Behav. Brain Res. 403, 113137.
Luft, A.R., Buitrago, M.M., 2005. Stages of motor skill learning. Mol. Neurobiol. 32, 205–216.
Mazere, J., Dilharreguy, B., Catheline, G., Vidailhet, M., Deffains, M., Vimont, D., Ribot, B., Barse, E., Cif, L., Mazoyer, B., Langbour, N., Pisani, A., Allard, M., Lamare, F., Guehl, D., Fernandez, P., Burbaud, P., 2021. Striatal and cerebellar vesicular acetylcholine transporter expression is disrupted in human DYT1 dystonia. Brain 144, 909–923.
McCool, M.F., Patel, S., Talati, R., Ragozzino, M.E., 2008. Differential involvement of M1-type and M4-type muscarinic cholinergic receptors in the dorsomedial striatum in task switching. Neurobiol. Learn. Mem. 89, 114–124.
Oleas, J., Yokoi, F., DeAndrade, M.P., Li, Y., 2015. Rodent models of autosomal dominant primary dystonia. In: LeDoux, M.S. (Ed.), Movement Disorders: Genetics and Models, Second ed. Academic Press Elsevier, New York, pp. 483–505.
Oleas, J., Yokoi, F., DeAndrade, M.P., Pisani, A., Li, Y., 2013. Engineering animal models of dystonia. Mov. Disord. 28, 990–1000.
Ozelius, L.J., Hewett, J.W., Page, C.E., Bressman, S.B., Kramer, P.L., Shalish, C., de Leon, D., Brin, M.F., Raymond, D., Corey, D.P., Fahn, S., Risch, N.J., Buckler, A.J., Gusella, J.F., Breakefield, X.O., 1997. The early-onset torsion dystonia gene (DYT1) encodes an ATP-binding protein. Nat. Genet. 17, 40–48.
Pappas, S.S., Darr, K., Holley, S.M., Cepeda, C., Mabrouk, O.S., Wong, J.M., LeWitt, T.M., Paudel, R., Houlden, H., Kennedy, R.T., Levine, M.S., Dauer, W.T., 2015. Forebrain deletion of the dystonia protein torsinA causes dystonic-like movements and loss of striatal cholinergic neurons. eLife 4, 08352.
Pappas, S.S., Li, J., LeWitt, T.M., Kim, J.K., Monani, U.R., Dauer, W.T., 2018. A cell autonomous torsinA requirement for cholinergic neuron survival and motor control. eLife 7, e36691.
Pisani, A., Bernardi, G., Ding, J., Surmeier, D.J., 2007. Re-emergence of striatal cholinergic interneurons in movement disorders. Trends Neurosci. 30, 545–553.
Prado, V.F., Roy, A., Kolisnyk, B., Gros, R., Prado, M.A., 2013. Regulation of cholinergic activity by the vesicular acetylcholine transporter. Biochem. J. 450, 265–274.
Richter, F., Richter, A., 2014. Genetic animal models of dystonia: common features and diversities. Prog. Neurobiol. 121, 91–113.
Scarduzio, M., Zimmerman, C.N., Jaunarajs, K.L., Wang, Q., Standaert, D.G., McMahon, L.L., 2017. Strength of cholinergic tone dictates the polarity of dopamine D2 receptor modulation of striatal cholinergic interneuron excitability in DYT1 dystonia. Exp. Neurol. 295, 162–175.
Seidler, R.D., 2004. Multiple motor learning experiences enhance motor adaptability. J. Cogn. Neurosci. 16, 65–73.
Sobreviela, T., Clary, D.O., Reichardt, L.F., Brandabur, M.M., Kordower, J.H., Mufson, E. J., 1994. TrkA-immunoreactive profiles in the central nervous system: colocalization with neurons containing p75 nerve growth factor receptor, choline acetyltransferase, and serotonin. J. Comp. Neurol. 350, 587–611.
Song, C.H., Bernhard, D., Bolarinwa, C., Hess, E.J., Smith, Y., Jinnah, H.A., 2013. Subtle microstructural changes of the striatum in a DYT1 knock-in mouse model of. Neurobiol. Dis. 54, 362–371.
Song, C.H., Bernhard, D., Hess, E.J., Jinnah, H.A., 2014. Subtle microstructural changes of the cerebellum in a knock-in mouse model of DYT1 dystonia. Neurobiol. Dis. 62, 372–380.
Song, C.H., Fan, X., Exeter, C.J., Hess, E.J., Jinnah, H.A., 2012. Functional analysis of dopaminergic systems in a DYT1 knock-in mouse model of dystonia. Neurobiol. Dis. 48, 66–78.
Sugimoto, H., Ikeda, K., Kawakami, K., 2014. Heterozygous mice deficient in Atp1a3 exhibit motor deficits by chronic restraint stress. Behav. Brain Res. 272, 100–110.
Xiao, J., Vemula, S.R., Xue, Y., Khan, M.M., Carlisle, F.A., Waite, A.J., Blake, D.J., Dragatsis, I., Zhao, Y., LeDoux, M.S., 2017. Role of major and brain-specific Sgce isoforms in the pathogenesis of myoclonus-dystonia syndrome. Neurobiol. Dis. 98, 52–65.
Yan, Z., Flores-Hernandez, J., Surmeier, D.J., 2001. Coordinated expression of muscarinic receptor messenger RNAs in striatal medium spiny neurons. Neuroscience 103, 1017–1024.
Yin, H.H., Mulcare, S.P., Hilario, M.R., Clouse, E., Holloway, T., Davis, M.I., Hansson, A. C., Lovinger, D.M., Costa, R.M., 2009. Dynamic reorganization of striatal circuits during the acquisition and consolidation of a skill. Nat. Neurosci. 12, 333–341.
Yokoi, F., Chen, H.X., Dang, M.T., Cheetham, C.C., Campbell, S.L., Roper, S.N., Sweatt, J. D., Li, Y., 2015a. Behavioral and electrophysiological characterization of Dyt1 heterozygous knockout mice. PLoS One 10, e0120916.
Yokoi, F., Dang, M.T., Li, J., Li, Y., 2006. Myoclonus, motor deficits, alterations in emotional responses and monoamine metabolism in epsilon-sarcoglycan deficient mice. J. Biochem. 140, 141–146.
Yokoi, F., Dang, M.T., Li, J., Standaert, D.G., Li, Y., 2011. Motor deficits and decreased striatal dopamine receptor 2 binding activity in the striatum-specific Dyt1 conditional knockout mice. PLoS One 6, 24539.
Yokoi, F., Dang, M.T., Li, Y., 2012. Improved motor performance in Dyt1 DeltaGAG heterozygous knock-in mice by cerebellar Purkinje-cell specific Dyt1 conditional knocking-out. Behav. Brain Res. 230, 389–398.
Yokoi, F., Dang, M.T., Liu, J., Gandre, J.R., Kwon, K., Yuen, R., Li, Y., 2015b. Decreased dopamine receptor 1 activity and impaired motor-skill transfer in Dyt1 DeltaGAG heterozygous knock-in mice. Behav. Brain Res. 279, 202–210.
Yokoi, F., Dang, M.T., Miller, C.A., Marshall, A.G., Campbell, S.L., Sweatt, J.D., Li, Y., 2009. Increased c-fos expression in the central nucleus of the amygdala and enhancement of cued fear memory in Dyt1 DeltaGAG knock-in mice. Neurosci. Res. 65, 228–235.
Yokoi, F., Dang, M.T., Mitsui, S., Li, J., Li, Y., 2008. Motor deficits and hyperactivity in cerebral cortex-specific Dyt1 conditional knockout mice. J. Biochem. 143, 39–47.
Yokoi, F., Jiang, F., Dexter, K., Salvato, B., Li, Y., 2020a. Improved survival and overt "dystonic" symptoms in a torsinA hypofunction mouse model. Behav. Brain Res. 381, 112451.
Yokoi, F., Oleas, J., Xing, H., Liu, Y., Dexter, K.M., Misztal, C., Gerard, M., Efimenko, I., Lynch, P., Villanueva, M., Alsina, R., Krishnaswamy, S., Vaillancourt, D.E., Li, Y., 2020b. Decreased number of striatal cholinergic interneurons and motor deficits in dopamine receptor 2-expressing-cell-specific Dyt1 conditional knockout mice. Neurobiol. Dis. 134, 104638.
Yokoi, F., Yang, G., Li, J., DeAndrade, M.P., Zhou, T., Li, Y., 2010. Earlier onset of motor deficits in mice with double mutations in Dyt1 and Sgce. J. Biochem. 148, 459–466.
Zanone, P.G., Kelso, J.A., 1997. Coordination dynamics of learning and transfer: collective and component levels. J. Exp. Psychol. Hum. Percept. Perform. 23, 1454–1480.
Zhang, L., Yokoi, F., Jin, Y.H., Deandrade, M.P., Hashimoto, K., Standaert, D.G., Li, Y., 2011. Altered dendritic morphology of purkinje cells in Dyt1 DeltaGAG knock-in and Purkinje cell-specific Dyt1 conditional knockout mice. PLoS One 6, 18357.